DC ELECTRICAL RESISTANCE MEASUREMENT IN COMPOSITE OF CUPRATE SUPERCONDUCTOR

A REPORT SUBMITTED TO

DEPARTMENT OF PHYSICS

NATIONAL INSTITUTE OF TECHNOLOGY, ROURKELA

BY

Kanchan Kumari Sharma (410PH2148)

&

Madhusmita Swain (410PH2151)

M.Sc. Physics

Under the supervision of

Prof. D. Behera

DEPARTMENT OF PHYSICS, NIT ROURKELA

DEPARTMENT OF PHYSICS

NATIONAL INSTITUTE OF TECHNOLOGY, ROURKELA

ROURKELA – 769 008

CERTIFICATE

This is to certify that the project report entitled "**DC electrical Resistance measurement in composite of cuprate Superconductor**" is submitted by **Miss Kanchan Kumari Sharma & Miss Madhusmita Swain** for partial fulfilment for the requirement towards the award of Master of Science degree in Physics at **NIT, Rourkela**. This is an authentic work carried out by them under my supervision and guidance in low temperature laboratory of Department of Physics.

To the best of my knowledge, the matter embodied in the thesis has not been submitted to any other University/Institute for the award of my degree.

Prof. D. Behera
Department of Physics

NIT, Rourkela

ACKNOWLEDGEMENT

On the submission of our thesis report title "**DC electrical resistance measurement in composite of cuprate superconductor**" We would like to thank our guide Prof **D. Behera** for his patience and his helpful discussion with us during the course of our work for the l year. We would like to thank **Miss Arpna Kujur**, **Miss Mousmibala Sahoo** for sharing ideas with us and helping in our project work.

We give sincere thanks to Department of Metallurgical and Material Science for extending all facilities to carry out the **XRD** and **SEM**.

We express heartiest thanks to all the faculty members of Department of Physics, NIT Rourkela who have made direct or indirect contribution towards the completion of this project.

It gives us an immense pleasure to thank all our friends and all the research scholars of the Dept. of Physics, NIT Rourkela for their constant inspiration.

KANCHAN KUMARI SHARMA

MADHUSMITA SWAIN

ABSTRACT

Bulk YBCO sample is prepared using solid state reaction route. Transport property of YBCO+ x NiO (x = 0.1, 0.7, 1 wt. %) is studied four probe method. Microstructural analysis is performed using scanning electron microscope and phase confirmation of YBCO powder is done by X-ray diffraction method. Data collected are computer controlled through automated programs. The transition temperature is affected on addition of NiO to YBCO. Both T_c and T_{c0} decrease immensely on addition of small quantity of magnetic material.

CONTENTS

CHAPTER-1

INTRODUCTION

1.1. Superconductivity:

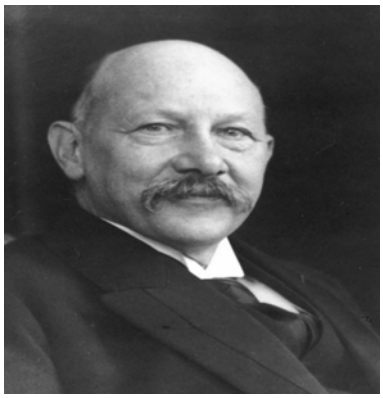

Kamerlingh Onnes (1911)

Superconductivity is a fascinating and challenging field of physics. It was first discovered by Dutch Physicist Heike Kamerlingh Onnes in 1911 at extremely low temperature near about absolute zero, by virtue of which electrical resistivity vanishes and they becomes diamagnetic in nature due to Meissners effect.

BCS THEORY:

BCS theory was proposed by bardeen,Cooper and Schrieffer in 1957. This was the first microscopic theory for superconductors (SCs). It is described superconductivity as a microscopic effect which is caused by a condensation of pairs of electrons into a boson like state. It is also used in nuclear physics which describe the interaction between nucleons in an atomic nucleus.

In 1957 Bardeen and Cooper assembled these ingredients and discovered such a theory which is named as BCS theory with the help of Robert Schrieffer. It was published first in april 1957. The demonstration had the phase transition of 2^{nd} order . This phase transition produced the Meissner effect. BCS is able to give an approximation for the quantum-mechanical many body state of the SCs system. This state is known as BCS state.

Attractive interaction between the electrons leads to a ground state which is separated the excited state by energy gap. Many properties such as thermodynamic properties, electromagnetic properties are the consequences of energy gap. Electron-phonon-electron or electron-lattice-electron interaction leads to an energy gap of magnitude of the order of 10 meV. The penetration depth and coherence length emerge as a natural consequence of BCS theory.

Superconductors are categorised based on the transition temperature and magnetic field penetration on the samples as Type- I SCs and Type- II SCs

1.2 Type-I Superconductors:-

Type-I SC obeys Meissners effect. It is also knows as soft superconductors. Very pure materials like lead, mercury, and tin etc are the type-I SC. Type-I SCs possess only one critical magnetic field H_c, below which the SC produces shielding currents that flow on the surface of the material expelling the magnetic field from its interior. In this condition the SC is in the Meissner state. Above Hc, the applied magnetic field penetrates completely into the interior of the material, disrupting the superconductors.

1.3 Type-II Superconductors:-

Type-II SCs are also known as hard superconductors as they can bear large magnetic field. High temperature superconductor such as $YBa_2Cu_3O_7$ is the type-II superconductors. Type-II SCs are characterised by two critical fields such as low critical field Hc_1 and high critical field Hc_2. Figure 1 shows the magnetic phase diagram for a type-II sc. Below Hc_1 the sc behaves likes a type I SC and it is the Meissner state.

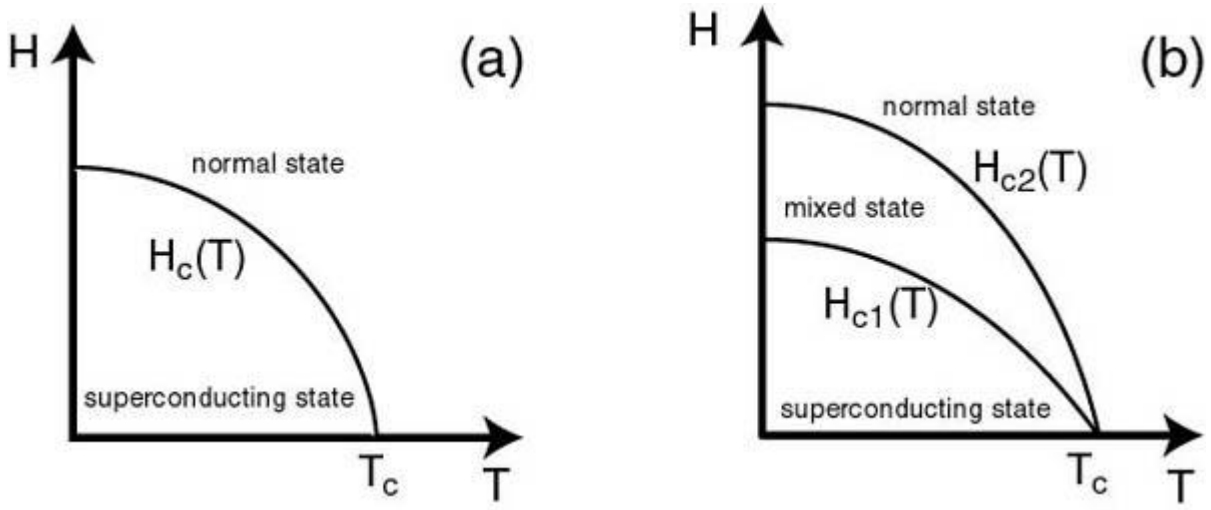

Fig.1: Magnetic phase diagram (H (T)) for (a) Type–I superconductors: one critical field Hc exists; (b) Type-II superconductors: where two critical fields exist (Lower critical field (Hc_1) & upper critical field (Hc_2))

The figure 2 below shows the behaviour of magnetic field to material. It obeys messier effect up to certain critical field Hc_1 at which magnetic flux begins to enter the SC and an upper critical field Hc_2 at which SC disappears.

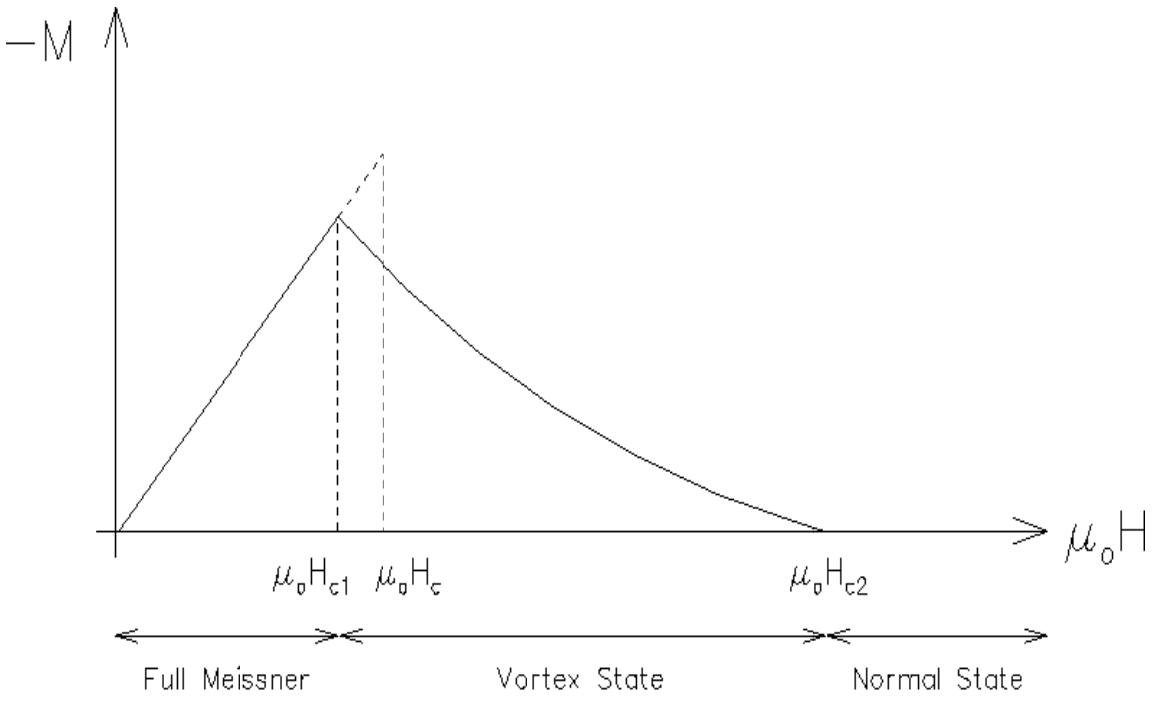

Fig. 2: M–H graph showing the different state of a type-II superconductor

1.4 PROPERTIES OF SUPERCONDUCTORS

Most of the physical properties of SC vary from material to material, such as the heat capacity and critical temperature, critical field, and critical current density.

1. **Zero electrical resistance**:-

To measure the resulting voltage V across the sample we take the electrical resistance of the sample to be placed it in an electric circuit in series with the current source I. The resistance of the sample is given by Ohm's law as $R=V/I$. If the voltage is zero, that means the resistance is zero and the sample is in superconducting state. The temperature at which the resistance of a superconductor is zero called the transition temperature.

2. Effect of magnetic field:-

At a particular range of temperature and field strength the superconducting state of a metal exit. Superconducting state will appear in the metal combination of when the temperature and field strength should be less than critical value. When the temperature of the specimen is raised above its Tc or sufficiently strong magnetic field is employed then the SC disappears.

$$H_c = H_o [1-(T/Tc)^2]$$

Hc is the maximum critical field strength at the temperature T. Ho is the maximum critical field strength occurring at absolute zero and Tc is the critical temperature.

3. Meissner effect:-

A superconductor with small or no magnetic field within it is said to be in the Meissner state. Meissner and Ochsenfeld measured the flux distribution outside tin and lead specimens which has been cooled below their transition temperature while in a magnetic field. They found their transition temperatures the specimens spontaneously became perfectly diamagnetic. Superconductor never has a flux density even when in applied magnetic field (B=0). At superconducting state when resistance is zero the magnetic behaviour is degined as diamagnetic.

4. Energy gap:-

The thermal properties of superconductors indicate that there is a gap in the distribution of energy levels available to the electrons, and so a finite amount of energy, designated as delta (Δ), must be supplied to an electron to excite it. This energy is maximum (designated Δ_0) at absolute zero and changes little with increase of temperature until the transition temperature is approached, where Δ_0 decreases to zero, its value in the normal state. The energy gap of a superconductor is very low ~ meV.

5. Effect of current:-

The magnetic field that causes a superconductor to become normal from a superconducting state is not necessarily by an external applied field. It may arise as a result of electric current flow in the conductor, the minimum current that can be passed in a simple without disturbing its superconductivity, is called critical current. If a wire of radius r of a Type 1 superconductor carries a current I, there is a surface magnetic field, $Hi = I/2\pi r$, associated with the current. If Hi exceeds Hc, the materials go normal.

6. Isotope effect:-

The critical temperature of superconductors varies with isotopic mass. The observation was first made by Maxwell and others, who used mercury isotope s. To give an idea of magnitude of the effect, for mercury T_c varies from 4.185 K to 4.146 K as the isotope mass M varies from 199.5 to 203.4. The isotope mass can enter in the process of the formation of the superconducting phases of the electron states only through the electron - phonons interaction.

7. Penetration depth:-

F. London and H.London described the meissner effect and zero resistivity by adding the two condition E= 0 (from the absence of resistivity) and B= 0 (from meissners effect) to Maxwell electromagnetic equation. According to them the applied field does not suddenly drop to zero at the surface of the superconductor, but decays exponentially according to the equation,

$$H = H_0 \exp(-x/\lambda)$$

Where H0 is the value of magnetic field at the surface and λ is a characteristics length known as the penetration depth; λ is the distance for H to fall from Ho to Ho/e.

APPLICATION:

- ✓ Production of sensitive magnetometer which is based on application of SQUID
- ✓ Fast digital circuits which are based on Josephson junction and quantum technology.
- ✓ Powerful superconducting electron magnets which are used in MRI, NMR and the focusing magnets which are used as practical accelerator.
- ✓ Low loss of power cables.
- ✓ RF and microwave filters.
- ✓ High sensitive particle detectors such as sensors.
- ✓ Electric motors and generators etc.

1.5 HIGH TEMPERATURE SUPERCONDUCTOR:

High temperature superconductors are marked by high critical current in magnetic field. High T_c superconductors are materials that have a superconducting transition temperature (T_c) above 30 K. From 1960 to 1980, 30 K was thought to be the highest theoretically possible T_c. In 1986 lanthanum based superconductor was discovered having T_c of 35 K for which Bednorz and K. Muller got the Noble prize in Physics in 1987. The figure 3 below shows the historical development of superconductivity from 1911. YBCO is one of the high temperature Cuprate SC followed by BSCCO, TBCCO, HBCCO. HBCCO having the highest T_c of 135 K. Remarkable feature is that Tc lies above the boiling point of liquid nitrogen 77 K.

The famous "high temperature superconductor" is the Yttrium barium copper oxide, often abbreviated as YBCO, is a crystalline chemical compound with the formula $YBa_2Cu_3O_7$,which is achieved prominence because it was the first material to achieve superconductivity above the boiling point of nitrogen i.e. 77K. All materials developed before 1986 became superconducting only at temperatures near the boiling points of liquid helium or liquid hydrogen (*T*b = 20.28 K) - the highest being Nb_3Ge at 23.2 K. The significance of the discovery of YBCO is the much lower cost of the refrigerant used to cool the material to below the critical temperature.

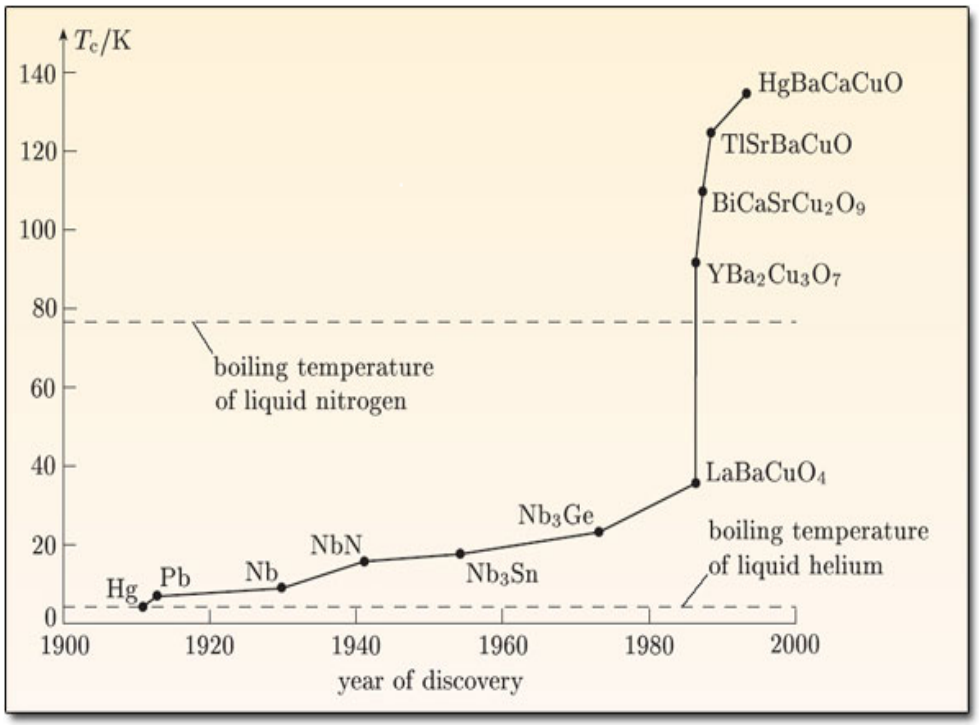

Fig.3: Time line of discovery of Superconductor

1.6 Structure of YBCO:-

The structure of YBCO is closely related to perovskite structure, and the structure of these compounds has been described as a distorted, oxygen deficient multi-layered perovskite structure. One of the properties of the crystal structure of oxide superconductors is an alternating multi-layer of CuO_2 planes with superconductivity taking place between these layers. The more layers of CuO_2 having higher *T*c. This structure causes a large anisotropy in normal conducting and superconducting properties, since electrical currents are carried by holes induced in the oxygen sites of the CuO_2 sheets. Yttrium barium copper oxide, often abbreviated YBCO, is a crystalline chemical compound with the formula $YBa_2Cu_3O_7$. YBCO crystallizes in a defect perovskite structure consisting of layers. The boundary of each layer is defined by planes of square planar CuO_4 units sharing 4 vertices (figure 4(a)). The planes can sometimes be slightly puckered perpendicular to these CuO_2 planes are CuO4 ribbons sharing 2 vertices. The Yttrium atoms are found between the CuO_2 planes, while the barium atoms are found between the CuO_4 ribbons and the CuO_2 planes. This structural feature is illustrated in the figure 4.

Although $YBa_2Cu_3O_7$ is a well-defined chemical compound with a specific structure and stoichiometry, materials with less than seven oxygen atoms per formula unit are non-stoichiometric compounds. The structure of these materials depends on the oxygen content. This non-stoichiometry is denoted by the $YBa_2Cu_3O_{7-x}$in the chemical formula. When $x = 1$, the O (1) sites in the Cu (1) layer are vacant and the structure is tetragonal. The tetragonal form of YBCO is insulating and does not super conduct. Increasing the oxygen content slightly causes more of the O (1) sites to become occupied. For $x < 0.65$, Cu-O chains along the *b*-axis of the crystal are formed. Elongation of the *b*-axis changes the structure to orthorhombic, with lattice parameters of $a = 3.82$, $b = 3.89$, and $c=11.68$ Å. Optimum superconducting properties occur when $x \sim 0.07$ and all of the O (1) sites are occupied with few vacancies.

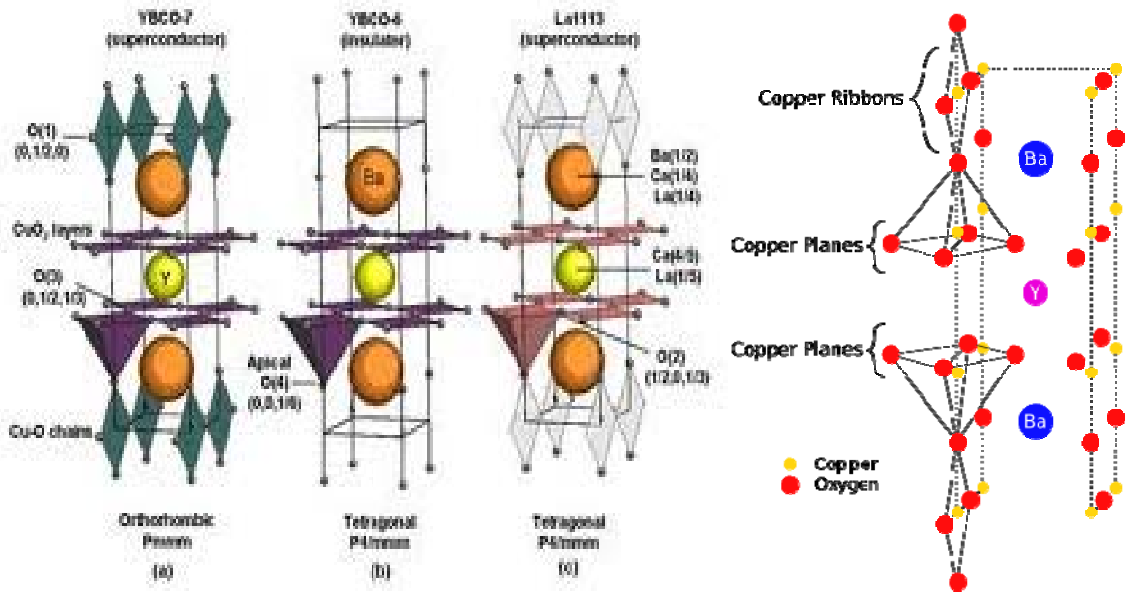

Fig. 4: orthorhombic and tetragonal phase of YBCO

1.7. STRUCTURE OF NICKEL OXIDE:

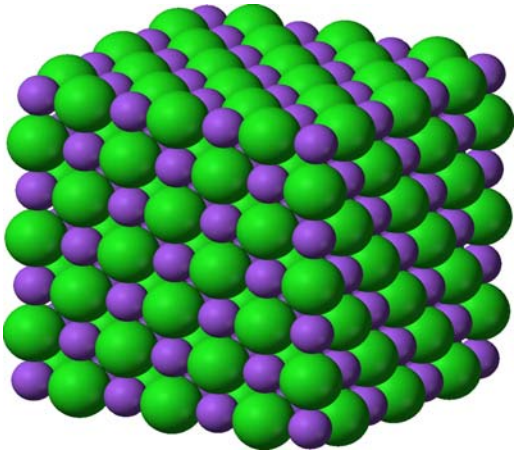

Fig. 5: Structure of NiO

Nickel oxide is a chemical compound with formula NiO. It is a notable as being the only well characterised oxide of nickel oxide. The mineralogical formula of NiO is bunsenite, is very rare. It is classified as a basic metal oxide. NiO adopts the Nacl structure with octahedral site. The simple structure is commonly known as rock salt structure. It is a non stoichometry compound. This stoichometry is accompanied by colour change with stoichometry correct NiO is green and the non-stoechometry correct NiO is black. This compound having molar mass 74.6g/mol. We use nickel oxide of 99% purity. It has melting point is 1984^0 C and density is 6.67gm/cm^3. NiO shows FCC structure [1].

APPLICATION:

- For making electrical ceramics such as thermistors and varistors e.g. ferrites.
- Pigments for ceramics, glass and glazes.
- It also acts with acids to form salts and other compounds e.g. nickel sulfamate for electroplating and nickel molybdate for hydrodesulfuriation catalyst.
- Gold dope nickel oxide films can be used as transparent electrodes.

CHAPTER-2

CHARACTERIZED TOOLS:

2.1. X-RAY DIFFRACTION:

X-ray diffraction is a very important non-destructive characterization technique, which is normally used to study the crystal structure of solids, including lattice constant, identifying unknown materials, orientation of single crystals, preferred orientation of thin films, defects, stress etc. This technique is based on the basic principle that a parallel monochromatic X-ray beam of wavelength 'λ' incident at an angle of θ is diffracted by a set of parallel planes of a crystal (Fig.), which is governed by Bragg's law:

$$2d \sin\theta = n\lambda \text{---------- (1)}$$

Where'd' is the interplanar spacing for a particular diffracting plane of the crystal.

In the diffraction pattern, peaks are observed which are characteristic to the crystal structure of the material, determines the diffraction pattern and the relative intensities between the different reflected lines. The Cu K_α emission (λ =0.154nm) from a copper target is the most common X-ray source for the diffraction measurement. Phase identification using X-ray diffraction depends on the position of the peaks in a diffraction pattern and the relative intensities of these peaks.

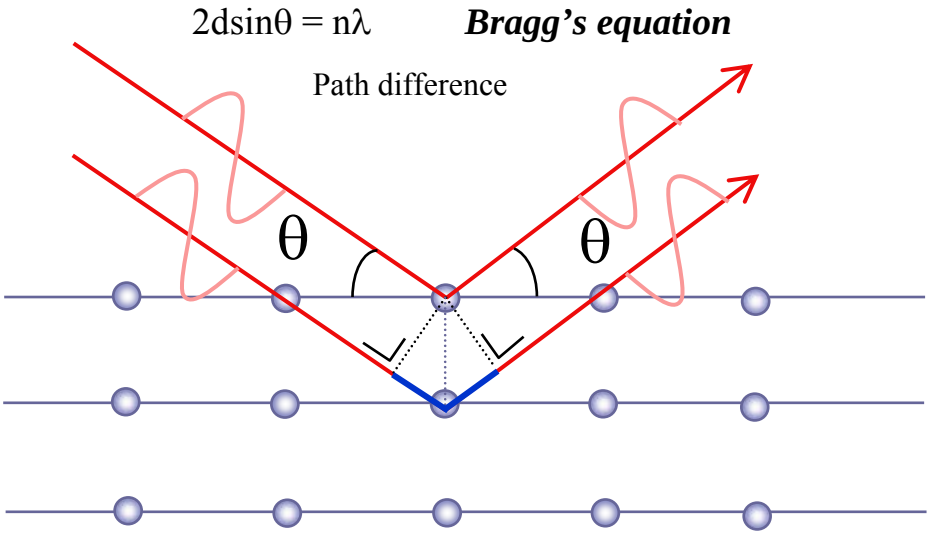

Fig.6: Bragg's diffraction

2.2. R-T MEASURMENT BY FOUR PROBE METHOD:

To determine the resistance by the ratio of voltage signal and a bais current four probe method is employed. The unit of voltage is nanovoltmeter. So the four probe contact is fundamental because it enables to minimise the spurious voltage due to current contact. The error due to voltage contact also minimised because the input impedance of the nano voltmeter is 1GΩ or higher. So the current flowing in voltage circuit between the sample and nanovoltmeter is lower than the bias current. The voltage drop is measured between the two probe labelled by means of a digital voltmeter.

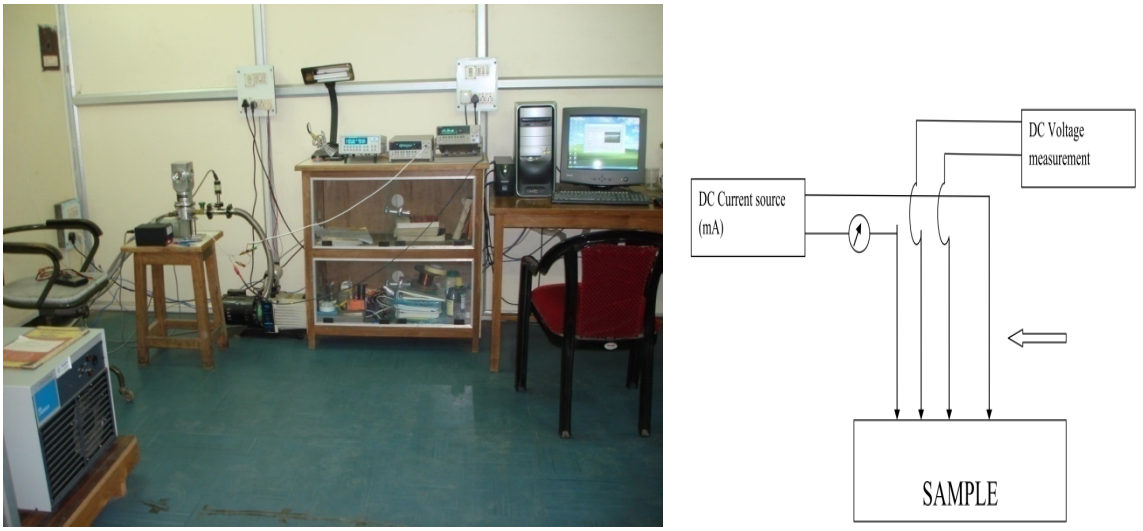

Fig.7: FOUR PROBE SETUP FOR RESISTANCE MEASUREMENT

2.3. SCANNING ELECTRON MICROSCOPE (SEM):-

Scanning electron microscopy is a type of electron microscope that images the sample surface by scanning with a high energy beam of electron raster scan pattern. The electrons interact with the atoms that make up the sample producing the signals that contain information about the sample surface's topography, composition and other properties such as electrical conductivity. The type of signals produced by SEM include secondary electrons, back scattering electrons (BSE), characteristics X-Ray, light (cathode luminescence), and specimen current and transmitted electrons. Secondary electron detectors are common in all SEM. The signals result from interaction of electron beam with atoms at or near the sample

surface. In the most common or standard detection mode, secondary electrons imaging (SEI) SEM can produce very high resolution images of the sample surface. SEM micrograph has a large depth of field yielding for the narrow electron beam. Back scattering electrons are the beam electrons that are reflected from the sample by elastic scattering. BSE are often used in analytical SEM along with the spectral mode from the characteristics X-rays. BSE images can provide information about the distribution of different elements in the sample because the intensities of BSE are related with the atomic number of the specimen.

CHAPTER-3

EXPERIMENTAL PROCEDURE:

PREPARATION OF YBCO:

The YBCO sample was prepared from the different precursor powder of high purity Alfa aeasor i.e. Y_2O_3 (99.99%), $BaCO_3$ (99.8%), CuO (99.995%).

The solid state reaction route involves following three steps:

1. Grinding

2. Calcination

3. Sintering

We have prepared YBCO by this solid state reaction route involving the chemical equation.

$$1/2Y_2O_3+2BaCO_3+3CuO+1/2O_2 \longrightarrow YBa_2Cu_3O_7+ 2CO_2$$

STEPS FOR PERPARATION:

- The appropriate amount of weighed chemicals in the ratio 1:2:3 were mixed in agate motor for about 2 to 3 hour to achieve homogeneous mixer.
- Then calcinations were done at 850^0c for about 10 hours. Then repeating this calcination for 4 times with intermediate grinding assured complete removal of CO_2 by the reaction and phase formation.
- Then the calcined black solid were regrounded for 1 hour. After grinding final pellets were made by applying pressure.
- Then the pellet was placed in an alumina crucible and sintered at 920^0C for 12 hours. Then they were slowly cooled at room temperature.
- After conformation of phase of YBCO sample we proceed for composite preparation.
- Now the mixture of YBCO and NiO (x = 0.1, 0.7, 1 wt. %) was grinded for about 1 hour.
- A series of polycrystalline sample of YBCO+ x NIO (x = 0.1, 0.7, 1 wt. %) were pressed into pellets. Then this pellet were sintered at 930°C and then cooled to hours.

- Then the temperature dependence resistance was measured using standard four probe method with a nanovoltmeter (Keithley-2182 A) current source (Keithley 6221) and also the scanning electron microscope characterization is done for the above prepared sample.

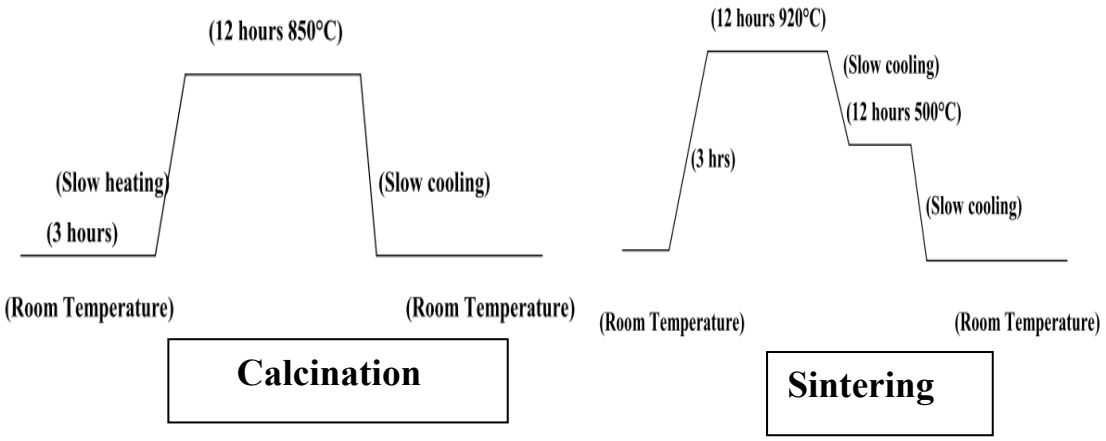

Fig.8: Heating Profile for calcination and Sintering

CHAPTER-4

RESULT AND DISCUSSION:

4.1. Phase identification:

Figure 1 shows the XRD patterns of YBCO pristine sample. The (00*l*) peaks of YBCO are observed. The diffraction pattern analysis of YBCO were indexed using Xpert Highscore software and the phases were confirmed to be orthorhombic at room temperature with a space group P_{mmm}. Few impurity peaks are also noticed. The major peak at (110) and (006) have been identified.

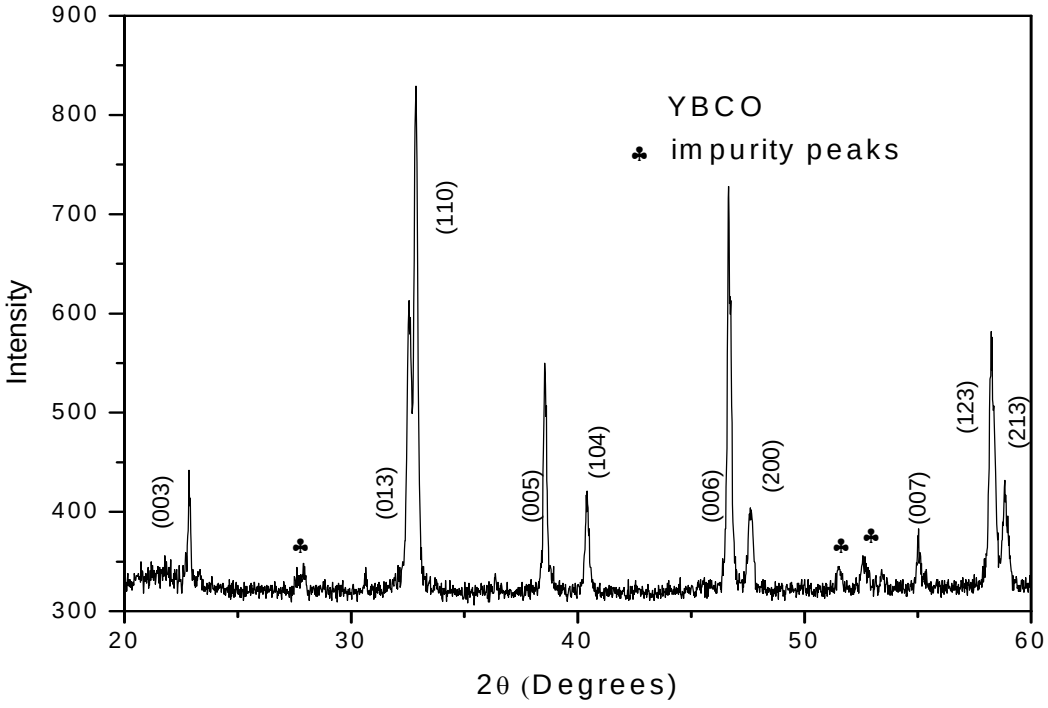

Fig.9: XRD pattern of YBCO

4.2. Microstructural Analysis:

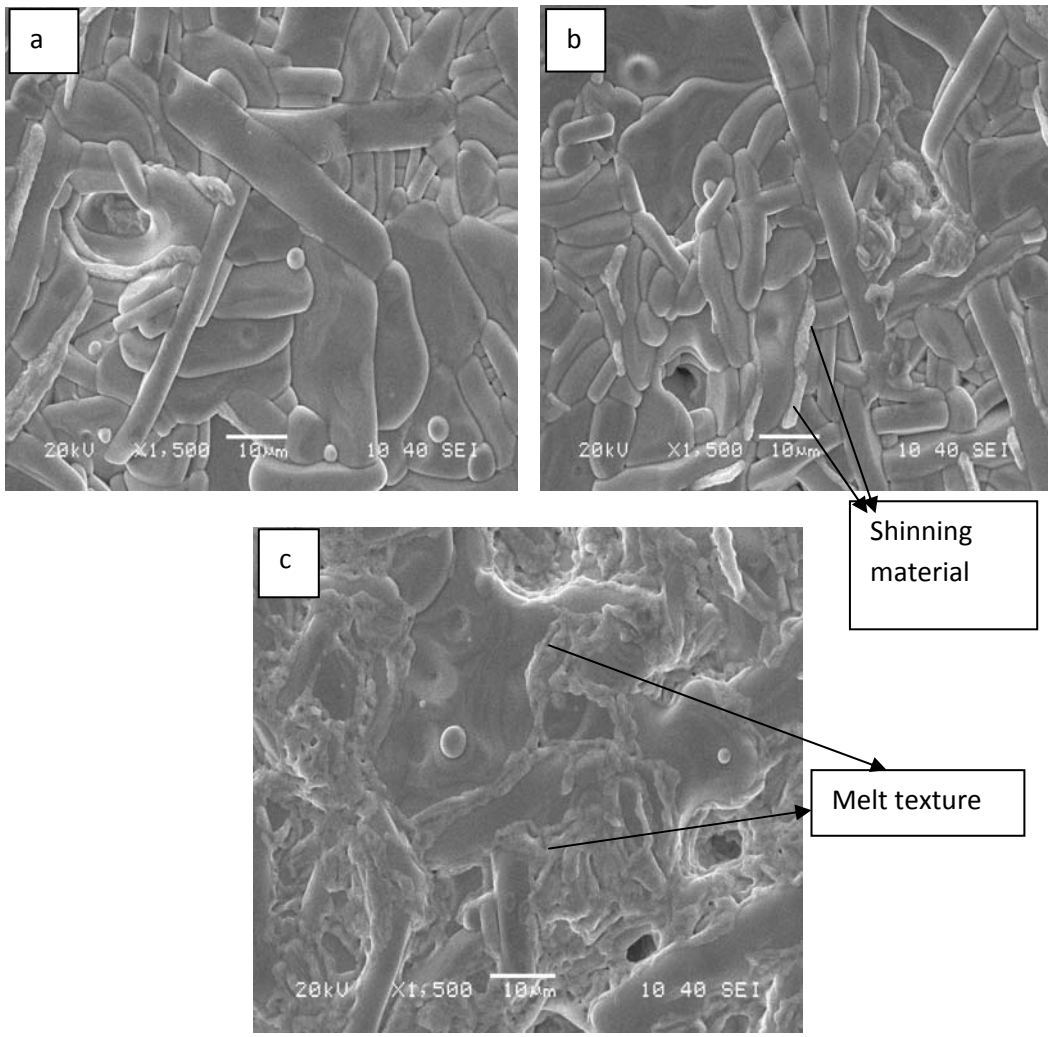

Fig.10: scanning Electron Microscope of (a) YBCO (b) YBCO+0.1 wt.%NiO (c)YBCO+1 wt.%NiO

The figure 10 shows SEM image of YBCO + x NiO (x = 0, 0.1,1 wt.%)). Rod shaped well distributed grains of varying length is identified in fig.10 (a). In this case the grains are well packed. Average grain length is up to 30µm and breath is up to 10µm. In fig.10 (b) there are grains consisting of some shining surface which may be due to melting of sample. In fig.10(c) we do not observe grains clearly because of a thick texture melt covering on the surface. Accelerating voltage used is 20 KV and magnification 10000X.

4.3. DC ELECTRICAL RESISTIVITY:

This figure 11 Shows the temperature dependent resistivity for composite sample (YBCO+ x % NiO), where x (0, 0.1, 0.7, 1 wt. %.). The room temperature resistivity increases with NiO addition. In this graph there are two regions. One is linear region showing metallic character and another is non-linear below 100 K.

The temperature derivative of the plots manifests sizeable information. From temperature derivative of resistivity graph a sharp peak is observed for YBCO and 0.1 wt% of NiO. However a bifurcation in peak occurs for higher wt. % of NiO giving a rise to double peaks. This is a clear indication of secondary phase present in the YBCO matrix. This peak is attributed to magnetic NiO. It is observed that T_c (onset of resistivity) and T_{C0} (global resistivity) decrease with addition of NiO. YBCO Pristine sample shows a transition $T_c \sim$ 92.75 K. Superconductivity first begins within the grains (intragranular regions) and then the grains boundaries are progressively coupled via weak link. NiO produces intragranular disturbances or electronic modification causing reduction of Tc and Tc0. Remarkable feature observed is the increment of transition width on mixing of NiO. The various parameters are evaluated and compiled in table 1.

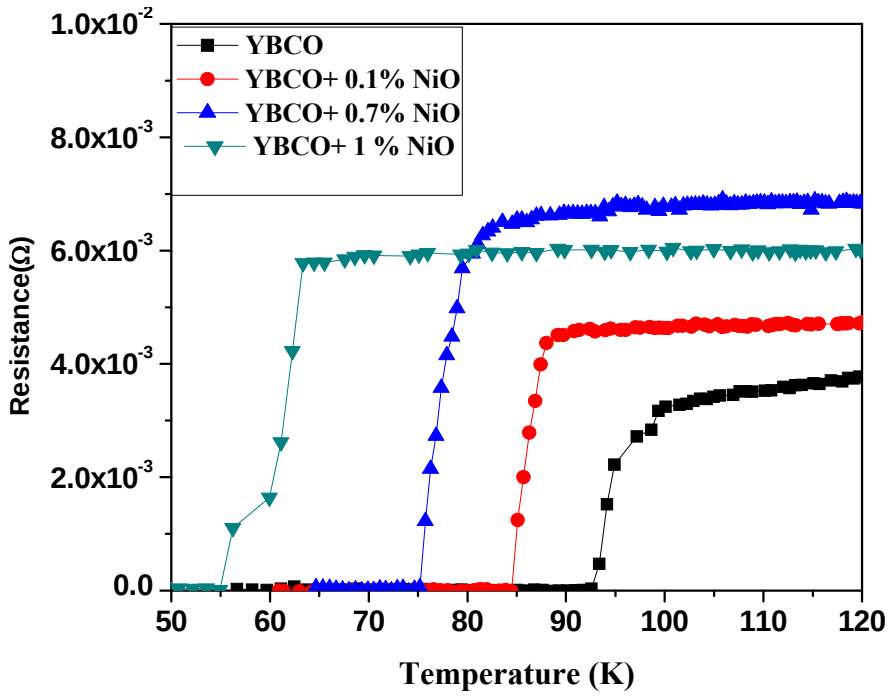

Fig.11:Temperature dependence resistance of YBCO+ x NiO composite

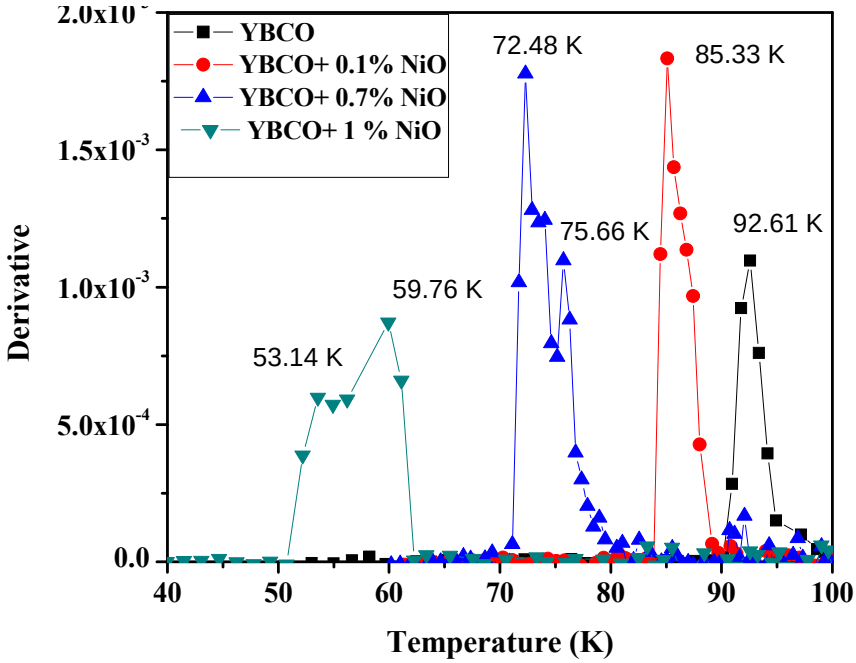

Fig.12: Temperature derivative of resistance of YBCO+ x NiO composite(x=0, 0.1%, 0.7 %, 1%)

Table 1: The various parameters associated with transition T_{c1}, T_{c2}, T_{c0} and resistance at 100 K (R_{100K}) temperature.

SAMPLE	Tc_0(K)	Tc_1(K)	Tc_2(K)	$R_{100K}\Omega$
YBCO	90.04	92.75	-	0.0032
YBCO+0.1%NiO	83.35	85.56	-	0.0046
YBCO+0.7%NiO	70.28	75.66	72.48	0.0062
YBCO+1%NiO	52.3	59.76	53.14	0.0059

CHAPTER-5

Conclusion:

The main findings of this project are highlighted below:

1. XRD confirms Phase identification of YBCO pristine sample with (00l) peaks dominating the plot. Few impurities peaks are also seen which remains unidentified.

2. Surface topology detected through SEM images reveals rectangular block of well defined grains formed in the samples. However melt texture covers the grains in YBCO+1%NiO making the grains invisible.

3. Temperature dependent resistance shows two regime one with linear nature and the other being non linear. The resistance at 100 K shows an increasing trend. The T_c parameter is highly affected when NiO enters the matrix of YBCO. Broadening is observed in the temperature derivative of resistance plot. T_{co} decreases as concentration increases attribting that the grain boundaries are affected much. Double peaks appear for 0.7 and 1 wt. % of the composite sample indicating the large inhomogeneities in T_c.

REFERENCES:

1. P. Mallick, D.C. Agarwal, Chandana Rath, R. Biswal, D. Behera, D.K. Avasthi, D. Kanjilal, P.V. Satyam, N.C. Mishra, Nuclear Instruments and Methods in Physics Research B 266 (2008) 3332–3335
2. C. H. Cheng and Y. Zhaoa, journal of applied physics, 93, (2003) 2292.
3. J. Joo, J.G. Kim, W. Nah, Superconductor Science and Technology, 11, (1998) 645.
4. D. Behera, S.K. Dash and N.C. Mishra, Phys. Lett. A 300 (2002) 529
5. John R Hull, Rep. Prog. Phys. 66 (2003) 1865.
6. Solid state physics by S.O.Pillai.
7. Introduction to Solid State Physics by C. Kittel.